Available online at www.sciencedirect.com
ScienceDirect
Journal of the European Ceramic Society 27 (2007) 4045–4049
www.elsevier.com/locate/jeurceramsoc

Crystal structure–polarization property relations in $(Sr_{0.5-x}Ca_x)Bi_{2.25}Na_{1.25}Nb_3O_{12}$ solid solutions

Atsushi Yokoi [a], Hirotaka Ogawa [a,*], Noriyuki Shimizu [b]

[a] *Faculty of Science and Technology, Meijo University, 1-501 Shiogamaguchi, Tempaku-ku, Nagoya 468-8502, Japan*
[b] *Department of Electrical and Electronic Engineering, Meijo University, 1-501 Shiogamaguchi, Tempaku-ku, Nagoya 468-8502, Japan*

Available online 7 May 2007

Abstract

The relationship between crystal structure and polarization properties of $(Sr_{0.5-x}Ca_x)Bi_{2.25}Na_{1.25}Nb_3O_{12}$ solid solutions was investigated in this study. A single phase of $(Sr_{0.5-x}Ca_x)Bi_{2.25}Na_{1.25}Nb_3O_{12}$ solid solutions was obtained over the whole composition range; the lattice parameters and the unit cell volume of $(Sr_{0.5-x}Ca_x)Bi_{2.25}Na_{1.25}Nb_3O_{12}$ solid solutions are linearly decreased with the Ca substitution for Sr. The decrease in the atomic distances of oxygen–oxygen bonds, which compose the equatorial plane, led to the decrease in the volume of the $Nb(1)O_6$ and $Nb(2)O_6$ octahedra caused by the Ca substitution for Sr. The covalency of the Nb(1)–O(1) bond increased in the composition range of 0–0.3, while that of the Nb(1)–O(1′) bond decreased in this composition range. The remanent polarizations (P_r) of the solid solutions were improved by the Ca substitution for Sr; the highest P_r value of 16 μC/cm^2 was obtained at $x = 0.3$. Thus, the variations in the P_r value caused by the Ca substitution for Sr may be attributed to the variations in the covalency of Nb(1)–O bonds in the $Nb(1)O_6$ octahedron, which is located the center of the pseudo-perovskite block. On the other hand, the coercive field (E_c) values of the solid solutions are in the order of approximately 45 kV/cm in the composition range of 0–0.5. Also, the Curie temperatures (T_c) of the solid solutions increased with increased the composition x; therefore, the increase in T_c value was connected with the decrease in the tolerance factor caused by the Ca substitution for Sr.

Keywords: Ferroelectric; Powders-solid state reaction; X-ray method

1. Introduction

Oxides of the Aurivillius family constitute an important class of materials because of their ferroelectric properties.[1] These materials are of interest for use in integrated circuit memories,[2] high temperature piezoelectric sensors[3] and electrooptic modulators.[4] Bismuth layer structured ferroelectrics (BLSFs) are generally formulated as $(Bi_2O_2)^{2+}(A_{m-1}B_mO_{3m+1})^{2-}$[5] BLSF compounds consist of an intergrowth between $(Bi_2O_2)^{2+}$ layers and $(A_{m-1}B_mO_{3m+1})^{2-}$ pseudo-perovskite blocks with m being the number of octahedra stacked along the direction perpendicular to the layers; therefore, A and B are the 12- and 6-fold coordination sites of the perovskite slab, respectively.[6]

In the research field of ferroelectric materials, there is an increasing demand for the development of alternative Pb-free ferroelectric materials to replace the $Pb(Zr_{1-x}Ti_x)O_3$ compounds.[7] Thus, the BLSF compounds as mentioned above are considered to be appropriate candidates as the Pb-free ferroelectric materials. One of bismuth-layered structures is $(Bi_2O_2)^{2+}(Sr_{0.5}Bi_{0.25}Na_{1.25}Nb_3O_{10})^{2-}$ with $m = 3$; the crystal structure of $Sr_{0.5}Bi_{2.25}Na_{1.25}Nb_3O_{12}$ ceramic is an orthorhombic structure with a $B2cb$ space group which corresponds to the BLSF compounds with $m = 3$. In recent work it was also reported that the tilting of oxygen octahedron in the pseudo-perovskite block plays an important role in improving the polarization properties of BLSF compounds.[8] In order to improve the polarization properties of $Sr_{0.5}Bi_{2.25}Na_{1.25}Nb_3O_{12}$ ceramic, the Ca substitution for Sr was performed and the $(Sr_{0.5-x}Ca_x)Bi_{2.25}Na_{1.25}Nb_3O_{12}$ solid solutions were synthesized; the relationships between crystal structure and polarization properties of the solid solutions were investigated in this study.

2. Experimental method

Synthesis of the $(Sr_{0.5-x}Ca_x)Bi_{2.25}Na_{1.25}Nb_3O_{12}$ solid solutions was conducted by the standard solid-state reaction method, using high purity $SrCO_3$, $CaCO_3$, Bi_2O_3, Na_2CO_3 and Nb_2O_5

* Corresponding author.
E-mail address: ogawah@ccmfs.meijo-u.ac.jp (H. Ogawa).

0955-2219/$ – see front matter © 2007 Elsevier Ltd. All rights reserved.
doi:10.1016/j.jeurceramsoc.2007.02.092

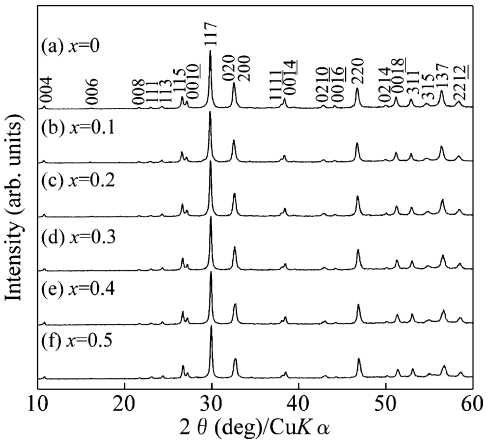

Fig. 1. XRPD patterns of $(Sr_{0.5-x}Ca_x)Bi_{2.25}Na_{1.25}Nb_3O_{12}$ solid solutions sintered at various temperatures for 2 h in air.

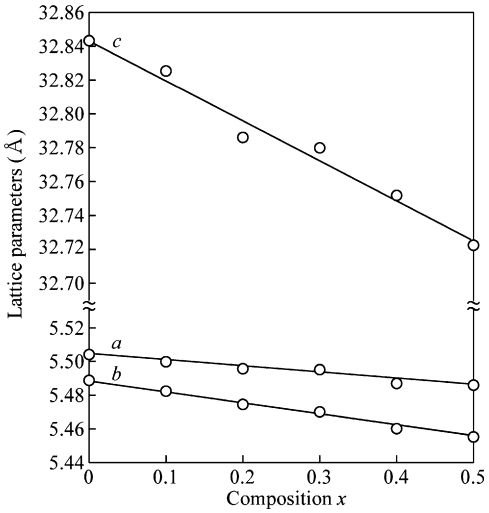

Fig. 2. Variation in lattice parameter of $(Sr_{0.5-x}Ca_x)Bi_{2.25}Na_{1.25}Nb_3O_{12}$ solid solutions as a function of composition x.

powders. These powders, weighed on the basis of the stoichiometric composition of $(Sr_{0.5-x}Ca_x)Bi_{2.25}Na_{1.25}Nb_3O_{12}$, were mixed and calcined at 800 °C for 4 h in air. Subsequently, the calcined powders were ground and mixed with a polyvinyl alcohol, and then pressed into a pellet of 12 mm in diameter and 3 mm in thickness under the pressure of 100 MPa. These pellets were sintered at 1100–1160 °C for 2 h in air. The crystalline phases of the crushed samples were identified by using the X-ray powder diffraction (XRPD) to ensure the formation of a single phase, and the crystal structure of the sample was refined with Rietveld analysis (RIETAN).[9,10] In order to evaluate the temperature dependence of the dielectric constants, these pellets were electroded with a platinum paste and fired at 950 °C for 30 min. The dielectric constants of the solid solutions were measured at 1 MHz with an LCR meter in the temperature range from room temperature to 850 °C. The *P–E* hysteresis loop was obtained at room temperature, using an aixACCT TF2000FE-HV ferroelectric test unit at 50 Hz.

3. Results and discussion

Fig. 1 shows the XRPD patterns of Ca-substituted $(Sr_{0.5-x}Ca_x)Bi_{2.25}Na_{1.25}Nb_3O_{12}$ solid solutions sintered at the various temperatures for 2 h in air. The XRPD results show that no secondary phase was detected throughout the entire composition range, and the peak shifts to the higher angle of 2θ are recognized with increasing the composition x. Thus, it is expected that the lattice parameters and the unit cell volume are varied by the Ca substitution for Sr; therefore, the lattice parameters and unit cell volume of the solid solutions are refined in terms of the Rietveld method, and the results are shown in Fig. 2 and Table 1. All the lattice parameters and the unit cell volume decrease in the composition range of 0–0.5; therefore, these results are predominantly due to the ionic radii of Ca (1.34 Å) and Sr (1.44 Å) ions, when the coordination number is 12.[11]

From these results, it was considered that the $(Sr_{0.5-x}Ca_x)Bi_{2.25}Na_{1.25}Nb_3O_{12}$ solid solutions satisfied Vegard's law, because of the linear variations in the lattice parameters of the solid solutions that were shown in the composition range of 0–0.5. Moreover, the difference in the lattice parameters, a and b, increased with increasing the composition x. The decrease in the lattice parameter, b, was larger than that in the lattice parameter, a, as shown in Fig. 2. Shimakawa et al. reported that the change from the orthorhombic phase to the tetragonal phase was attributed to the lattice distortion.[12] In order to clarify the lattice distortion caused by the Ca substitution for Sr, the orthorhombicity, which is defined as $2(a-b)/(a+b)$,[12] was calculated in this study. The orthorhombicity of the solid solutions increases linearly with increasing the composition x as listed in Table 2; therefore, the increase in the orthorhombicity may be attributed to the increase in the lattice distortion. Moreover, it is considered that the variations in the orthorhombicity are related to the tolerance factor. Several researchers have used the tolerance factor to

Table 1
Lattice parameters, unit cell volume and reliability factors of Rietveld analysis for $(Sr_{0.5-x}Ca_x)Bi_{2.25}Na_{1.25}Nb_3O_{12}$ ($x = 0$–0.5) ceramics

x	Lattice parameter (Å)			Unit cell volume (Å^3)	R_{wp}	R_p	s
	a	b	c				
0	5.5083(6)	5.4929(7)	32.8434(33)	993.73(21)	8.41	6.41	1.75
0.1	5.5041(5)	5.4866(7)	32.8255(31)	991.31(19)	9.01	6.96	1.58
0.2	5.4998(6)	5.4786(7)	32.7860(34)	987.90(20)	9.50	7.28	1.78
0.3	5.4994(5)	5.4746(6)	32.7799(34)	986.91(18)	9.35	7.20	1.75
0.4	5.4912(6)	5.4643(9)	32.7518(39)	982.74(23)	10.8	8.28	1.89
0.5	5.4901(6)	5.4596(7)	32.7225(40)	980.82(21)	10.2	7.84	1.90

Table 2
Variations in orthorhombicity and tolerance factor of $(Sr_{0.5-x}Ca_x)Bi_{2.25}Na_{1.25}Nb_3O_{12}$ solid solutions

Composition (x)	Orthorhombicity ($\times 10^{-3}$)	Tolerance factor
0	2.79	0.96752
0.1	3.19	0.96578
0.2	3.85	0.96405
0.3	4.52	0.96232
0.4	4.90	0.96058
0.5	5.58	0.95885

explain the stability of perovskites[13]; the tolerance factor is calculated from the following equation[13]:

$$t = \frac{R_A + R_O}{\sqrt{2}(R_B + R_O)} \quad (1)$$

where R_A, R_B and R_O are the radii of the A- and B- and the O-ions, respectively. The t values of the solid solutions varied from 0.96752 to 0.95885 in the composition range of 0–0.5 as listed in Table 2; therefore, it is considered that the structural distortion in the pseudo-perovskite block is increased by the Ca substitution for Sr. Such variations in the orthorhombicity and the tolerance factor as described above may have an influence on the polarization properties of $(Sr_{0.5-x}Ca_x)Bi_{2.25}Na_{1.25}Nb_3O_{12}$ solid solutions.

The crystal structure of $Sr_{0.5}Bi_{2.25}Na_{1.25}Nb_3O_{12}$ ceramic consists of the $(Bi_2O_2)^{2+}$ layers and $(Sr_{0.5}Bi_{0.25}Na_{1.25}Nb_3O_{12})^{2-}$ pseudo perovskite blocks with triple perovskite layers; the schematic diagram of $Nb(1)O_6$ and $Nb(2)O_6$ octahedra are shown in Fig. 3.

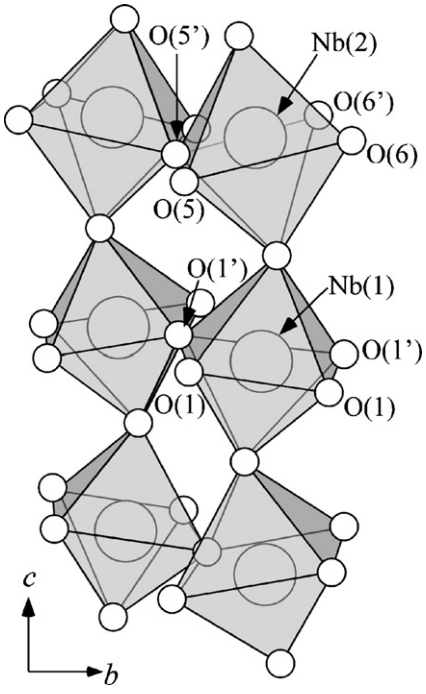

Fig. 3. Schematic diagrams of crystal structure of $Nb(1)O_6$ and $Nb(2)O_6$ octahedra in pseudo-perovskite block.

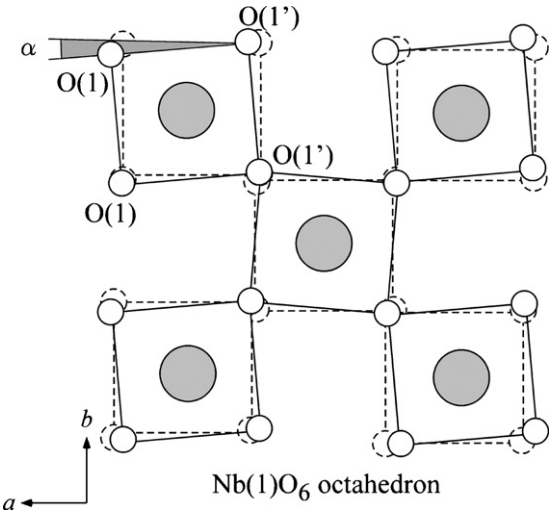

Fig. 4. Schematic diagram of $Nb(1)O_6$ octahedron in pseudo-perovskite block along c-axis.

Since it has known that the ferroelectricity of BLSFs compounds arises mainly from the perovskite blocks,[14] we focused on the $Nb(1)O_6$ and $Nb(2)O_6$ octahedra in the pseudo-perovskite block. Fig. 4 gives the schematic representation of $Nb(1)O_6$ octahedron in the pseudo-perovskite block along the c-axis. Several researchers have reported that the rotation of oxygen octahedron in the a–b plane exerts an influence on the polarization property[15]; the variation in the rotation angle (α) as shown in Fig. 4 is proportional to the Curie temperature. In this study, it was recognized that the variations in the orthorhombicity of the solid solutions was related to the tolerance factor caused by the Ca substitution for Sr. Thus, the variations in the axial ratio may be associated with the Curie temperature, because the increase in the axial ratio increases the rotation angle (α). From these results, it is expected that the Curie temperatures of the solid solutions are increased by the Ca substitution for Sr. Moreover, the volumes of the $Nb(1)O_6$ and $Nb(2)O_6$ octahedra in the pseudo-perovskite block were slightly decreased by the Ca substitution for Sr. Therefore, it is considered that the volumes of these octahedra may be attributed to the variations in the atomic distances of these octahedra. In order to clarify the variations in the atomic distances of $Nb(1)O_6$ and $Nb(2)O_6$ octahedra caused by the Ca substitution for Sr, those of the octahedra, which were calculated from the results of the Rietveld analysis, were listed in Table 3. The atomic distances of oxygen–oxygen ions in the

Table 3
Atomic distances of $Nb(1)O_6$ and $Nb(2)O_6$ octahedra

Atomic distances (Å)	$(Sr_{0.5-x}Ca_x)Bi_{2.25}Na_{1.25}Nb_3O_{12}$ solid solutions		
	$x=0$	$x=0.3$	$x=0.5$
O(1)–O(1)′	2.7701	2.7656	2.7609
O(1)–O(1)	2.4813	2.4732	2.4664
O(1)′–O(1)′	3.0685	3.0583	3.0500
O(6)–O(6)′	2.7678	2.7633	2.7586
O(6)–O(5)	2.9822	2.9725	2.9645
O(6)′–O(5)′	2.6952	2.6865	2.6793
O(5)′–O(5)	2.8128	2.8080	2.8032

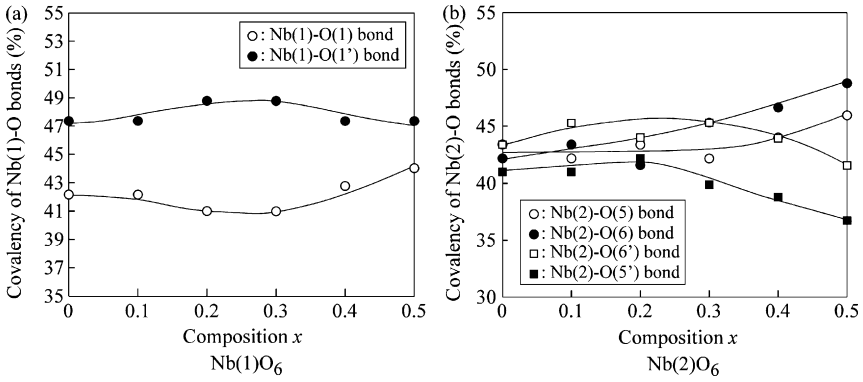

Fig. 5. Variation in covalency of $(Sr_{0.5-x}Ca_x)Bi_{2.25}Na_{1.25}Nb_3O_{12}$ solid solutions as a function of composition x.

equatorial plane of $Nb(1)O_6$ and $Nb(2)O_6$ octahedra decreased, depending on the composition x. Consequently, it is considered that the variations in these atomic distances lead to the decrease in the volumes of these octahedra. Therefore, the covalency of Nb–O bonds over the whole composition range were calculated by using the refined bond length. The relationship between the covalency and the bond length is given by two equations[16–18]:

$$s = \left(\frac{R}{R_1}\right)^{-N} \tag{2}$$

and

$$f'_c = as^M \tag{3}$$

where s is the bond strength, R is the refined bond length, and R_1, N, a and M are the empirically determined parameters, which reported by Brown et al.[17,18] The covalencies of Nb–O bonds in the $Nb(1)O_6$ and $Nb(2)O_6$ octahedra caused by the Ca substitution for Sr are shown in Fig. 5. As for the $Nb(1)O_6$ octahedron, the covalency of Nb(1)–O(1) bond increased in the composition range of 0–0.3, whereas that of Nb(1)–O(1′) bond decreased in such the composition range. In the case of $Nb(2)O_6$ octahedron, the covalencies of Nb(2)–O(6′) and Nb(2)–O(5′) bonds remained unaltered, though the covalencies of these bonds decreased at the compositions higher than $x = 0.3$.

On the other hand, the covalencies of Nb(2)–O(5) and Nb(2)–O(6) bonds were increased by the Ca substitution for Sr. It is expected that the variations in the covalencies of Nb–O bonds may be concerned with the changes in the polarization properties of the solid solutions caused by the Ca substitution for Sr.

Fig. 6 shows the P–E hysteresis loops of the $(Sr_{0.5-x}Ca_x)Bi_{2.25}Na_{1.25}Nb_3O_{12}$ solid solutions measured at room temperature. The well-saturated hysteresis loop was obtained at $x = 0.3$; therefore, the Ca substitution for Sr was effective in improving the P_r value of the solid solutions. Fig. 7 also provides the remanent polarization (P_r) and the coercive field (E_c) of the solid solutions as a function of composition x. The P_r values of the solid solutions increased from 12.4 to 16 μC/cm² in the composition range of 0–0.3, while the values of the solid solutions drastically decreased at the compositions higher than $x = 0.4$. On the other hand, the E_c values of the solid solutions remains the constant value of approximately 45 kV/cm in the composition range of 0–0.5. Consequently, the Ca substitution for Sr was not effective in improving the E_c value in this system. From these results, it is considered that the variations in the P_r value of the solid solutions may be connected with the difference in the covalencies of Nb(1)–O(1) and Nb(1)–O(1′) bonds, because the difference in the covalencies of Nb-O bonds may lead the tilting in the $Nb(1)O_6$ octahedron, which is located in the center in the pseudo-perovskite block.

The temperature dependence of the dielectric constant of the $(Sr_{0.5-x}Ca_x)Bi_{2.25}Na_{1.25}Nb_3O_{12}$ solid solutions measured at a frequency of 1 MHz is shown in Fig. 8. It has been known that the BLSF compounds, which contain the Na ion, show an abnormal variation in the temperature dependence of the dielectric constant.[19] As for the Ca-substituted

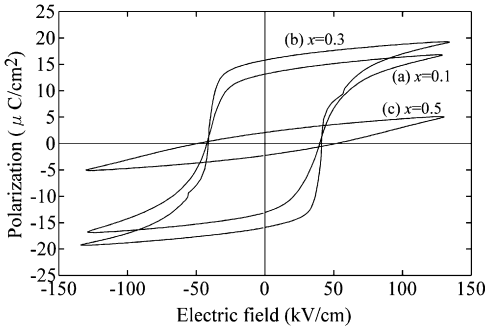

Fig. 6. Hysteresis loops of $(Sr_{0.5-x}Ca_x)Bi_{2.25}Na_{1.25}Nb_3O_{12}$ solid solutions measured at maximum applied field (E_m) of about 130 kV/cm.

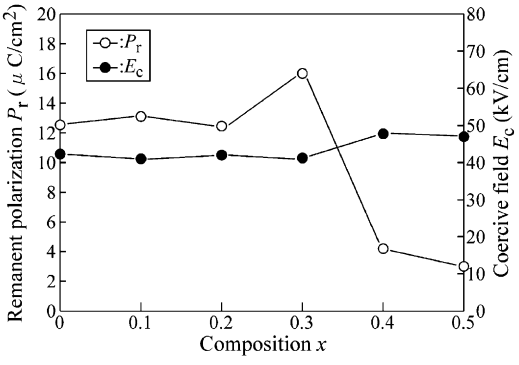

Fig. 7. Effects of Ca substitution for Sr on remanent polarization (P_r) and coercive field (E_c) of $(Sr_{0.5-x}Ca_x)Bi_{2.25}Na_{1.25}Nb_3O_{12}$ solid solutions.

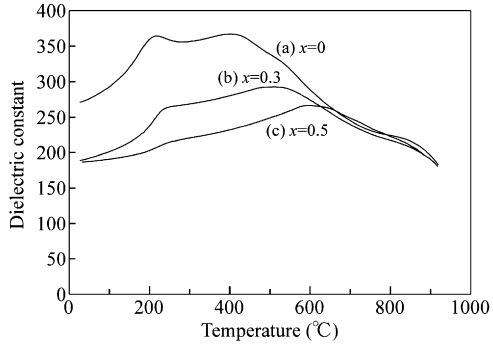

Fig. 8. Temperature dependence of dielectric constant for $(Sr_{0.5-x}Ca_x)Bi_{2.25}Na_{1.25}Nb_3O_{12}$ solid solutions measured at frequency of 1 MHz.

$(Sr_{0.5-x}Ca_x)Bi_{2.25}Na_{1.25}Nb_3O_{12}$ solid solutions, abnormal variations in the dielectric constant were recognized over the whole composition range. The Curie temperature (T_c) of the solid solutions also increased from 402 to 595 °C, depending on the composition x. It has been known that the variations in the T_c values of BLSF compounds are related to the tolerance factor. As mentioned earlier, the tolerance factor of the solid solutions decreased from 0.96752 to 0.95885 with increasing the composition x, as listed in Table 2. Thus, it is considered that the structural distortion in the pseudo-perovskite block is increased by the Ca substitution for Sr. From these results, the decrease in the T_c values is connected to the increase in the t values caused by the Ca substitution for Sr.

4. Conclusion

The effects of the Ca substitution for Sr on the polarization properties and the crystal structure of $(Sr_{0.5-x}Ca_x)Bi_{2.25}Na_{1.25}Nb_3O_{12}$ solid solutions were investigated in this study. From the results of XRPD, a secondary phase was not detected over the whole composition range. The lattice parameters and the unit cell volumes of $(Sr_{0.5-x}Ca_x)Bi_{2.25}Na_{1.25}Nb_3O_{12}$ solid solutions decreased, depending on the composition x. Also, the volumes of $Nb(1)O_6$ and $Nb(2)O_6$ octahedra slightly decreased with the decreased atomic distances of the oxygen–oxygen bonds, which composed the equatorial plane. The P_r values of the solid solutions improved with the Ca substitution for Sr and the highest P_r value of 16 μC/cm^2 was obtained at $x = 0.3$. The variations in the P_r values may be attributed to the covalencies of Nb(1)–O bonds in the $Nb(1)O_6$ octahedron, which locates the center in the pseudo-perovskite block. On the other hand, the E_c values of the solid solutions were on the order of approximately 45 kV/cm. Furthermore, the increases in the Curie temperature of the $(Sr_{0.5-x}Ca_x)Bi_{2.25}Na_{1.25}Nb_3O_{12}$ solid solutions is attributed to the decrease in the tolerance factor of the pseudo-perovskite block.

References

1. Aurivillius, B., Structure of $Bi_4Ti_3O_{12}$. *Arkh. Khemi.*, 1950, **1**, 499–512.
2. Scott, J. F., Ross, F. M., Paz de Araujo, C. A., Scott, M. C. and Huffman, M., Structure and device characteristics of $SrBi_2Ta_2O_9$-based nonvolatile random-access memories. *MRS Bull.*, 1996, **21**, 33–39.
3. Reaney, I. M., Roulin, M., Shulman, H. S. and Setter, N., In situ observations of octahedral tilt transitions in strontium bismuth titanate layered perovskites. *Ferroelectrics*, 1995, **165**, 295–305.
4. Xu, Y., *Ferroelectric Materials and their Applications*. Amsterdam, North-Holland, 1991.
5. Wu, Y., Forbess, K. J., Seraji, S., Limmer, S. J., Chou, T. P., Nguyen, C. *et al.*, Doping effect in layer structured $SrBi_2Nb_2O_9$ ferroelectrics. *J. Appl. Phys.*, 2001, **90**, 5296–5302.
6. Kobayashi, T., Noguchi, Y. and Miyayama, M., Polarization properties of superlattice-structured $Bi_4Ti_3O_{12}$–$BaBi_4Ti_4O_{15}$ single crystals and ceramics: comparison with $Bi_4Ti_3O_{12}$ and $BaBi_4Ti_4O_{15}$. *Jpn. J. Appl. Phys.*, 2004, **43**, 6653–6657.
7. Kakimoto, K., Masuda, I. and Ohsato, H., Lead-free $KNbO_3$ piezoceramics synthesized by pressure-less sintering. *J. Eur. Ceram. Soc.*, 2005, **25**, 2719–2722.
8. Noguchi, Y., Miyayama, M. and Kudo, T., Direct evidence of A-site deficient strontium bismuth tantalate and its enhanced ferroelectric properties. *Phys. Rev. B*, 2001, **63**, 2141021–2141025.
9. Rietveld, H. M., Profile refinement method for nuclear and metal urinates. *J. Appl. Crystallogr.*, 1969, **2**, 65–71.
10. Izumi, F., In *Rierveld Method*, ed. R. Young. Oxford University Press, Oxford, 1993 [Chapter 13].
11. Shannon, R. D., Dielectric polarizabilities of ions in oxides and fluorides. *J. Appl. Phys.*, 1993, **73**, 348–366.
12. Shimakawa, Y., Kudo, Y., Tauchi, Y., Asano, H., Kamiyama, T., Izumi, F. *et al.*, Crystal and electronic structures of $Bi_{4-x}La_xTi_3O_{12}$ ferroelectric materials. *Appl. Phys. Lett.*, 2001, **79**, 2791–2793.
13. Bhide, S. V. and Virkar, A. V., Stability of $AB'_{1/2}B''_{1/2}$ O_3-type mixed perovskite proton conductors. *J. Electrochem. Soc.*, 1999, **146**, 4386–4392.
14. Miyayama, M. and Noguchi, Y., Polarization properties and oxygen-vacancy distoribution of $SrBi_2Ta_2O_9$ ceramics modified by Ce and Pr. *J. Eur. Ceram. Soc.*, 2005, **25**, 2477–2482.
15. Noguchi, Y., Shimizu, H., Miyayama, M., Oikawa, K. and Kamiyama, T., Ferroelectric properties and structure distortion in A-site-modified $SrBi_2Ta_2O_9$. *Jpn. J. Appl. Phys.*, 2001, **40**, 5812–5815.
16. Brese, N. E. and O'Keeffe, M., Bond-valence parameters for solids. *Acta Cryst. B*, 1991, **47**, 192–197.
17. Brown, I. D. and Shannon, R. D., Empirical bond-strength-bond-length curves for oxides. *Acta Cryst. A*, 1973, **29**, 266–282.
18. Brown, I. D. and Wu, K. K., Empirical parameters for calculating cation-oxygen bond valences. *Acta Cryst. B*, 1976, **32**, 1957–1959.
19. Takenaka, T., Gotoh, T., Mutoh, S. and Sasaki, T., A new series of bismuth layer-structured ferroelectrics. *Jpn. J. Appl. Phys.*, 1995, **34**, 5384–5388.